



# An investigation of the influence of integration of steel heat treatment and brazing process on the microstructure and performance of vacuum-brazed cemented carbide/steel joints

W. Tillmann<sup>1</sup> · T. Ulitzka<sup>1</sup> · L. Dahl<sup>2</sup> · L. Wojarski<sup>1</sup> · H. Ulitzka<sup>1</sup>

Received: 4 November 2021 / Accepted: 1 February 2022 / Published online: 28 February 2022  
© The Author(s) 2022

## Abstract

Cemented carbides are commonly brazed to transformation hardening tool steels without taking a proper and adequate steel heat treatment into account. This publication shows the limits and possibilities of integrating a steel heat treatment, including a quenching process, into a vacuum brazing process. Therefore, copper-based filler metals are selected to ensure the steel component's high and homogenous hardness and supply a high joint quality. In this context, the aimed steel hardness was chosen in the range between 400 and 440 HV1 based on industrial experiences. This specific hardness range for the steel component was set to avoid wear of machining tools in subsequent machining steps if the steel hardness is too high and to prevent wear and deformation of the tool itself in case of a steel hardness too low. When using the transformation hardening tool steel 1.2344, the obtained shear strength values did not exceed a threshold of 20 MPa which can be attributed to the required N<sub>2</sub>-quenching from brazing respectively solution annealing temperature. However, the steel components featured a hardness of 527.1 HV1 for the specimens brazed with pure copper at 1100 °C and 494.0 HV1 for those brazed with a CuGeNi filler metal at 1040 °C. This publication also shows an alternative route to manufacture long-lasting tools with a cemented carbide/steel joint by applying the difficult to wet and not well researched, but for many other reasons very suitable precipitation hardening maraging steel. Especially, the comparable low coefficient of thermal expansion (CTE) and the capability of the lath martensite to compensate large amounts of externally imposed stresses during the austenite-to-martensite transformation as well as the cooling rate independent of the hardening mechanism of the maraging steel and a pre-applied nickel coating including the corresponding diffusion processes are responsible for a sound joint with a shear strength > 300 MPa. Moreover, the subsequent tempering process at 580 °C for 3 h provides the maraging steel joining partner with a hardness of 426.6 ± 6.0 HV1.

**Keywords** Vacuum brazing · Cemented carbide · Heat treatment · Maraging steel · Microstructure · Joint strength

## 1 Introduction

The widely spread induction brazing process under argon atmosphere is used to fabricate high-strength and long-lasting cemented carbide/steel joints [1]. A local change of the usually pre-hardened tool steel microstructure and thus an

uncontrolled hardening and embrittlement is tolerated within this joining process to achieve a firm bond between the joining partners [2, 3]. Another promising manufacturing route to fabricate long-lasting, wear-resistant cemented carbide/steel tools is applying a vacuum brazing process. Due to the vacuum brazing process characteristics, the heat transfer into the specimens is initiated comprehensively by the heat transfer modes convection (0.5 W/cm<sup>2</sup>), thermal radiation (8 W/cm<sup>2</sup>), and thermal conduction (20 W/cm<sup>2</sup>). These heat transfer modes result in significantly lower heating and cooling rates compared to brazing processes with a local heat input like induction (30,000 W/cm<sup>2</sup>) and laser brazing (1,000,000 W/cm<sup>2</sup>) [4]. The uniform exposure of the joining partners is challenging because the occurring temperatures will influence the microstructure and the mechanical

---

Recommended for publication by Commission XVII—Brazing, Soldering and Diffusion Bonding

---

✉ T. Ulitzka  
tim.ulitzka@tu-dortmund.de

<sup>1</sup> Institute of Materials Engineering, TU Dortmund University, Dortmund, North Rhine-Westphalia, Germany

<sup>2</sup> Sandvik Coromant, Sandviken, Sweden

properties of the pre-heat-treated steel. In this context, the optimal temperature control for brazing cemented carbide to steel directly conflicts with the recommended procedure for quenching and tempering transformation hardening tool steels. A controlled low cooling rate is critical to sufficiently reduce the already high thermal-induced residual stresses. By slowly cooling down from brazing temperature to room temperature, the stressed fillet, which has absorbed and relieved the thermally induced relative movements of the joining partners by plastic deformation, can be relaxed [5]. However, a sufficiently high cooling rate is essential for increasing hardness, strength, and stiffness and for avoiding undesirable intermediate phase mixtures (e.g., pearlite or bainite) in the steel [6]. Generally, brazed cemented carbide/transformation hardening tool steel joints are either cooled freely [7], in a controlled manner with a cooling rate between 3 and 15 °C/min [8–10], or the authors do not address the temperature–time profile during the cooling phase at all [11–14]. The focus, which is generally put on the braze joint properties as well as the lack of consideration regarding the ideal steel heat treatment and properties, leaves room for further developments in terms of manufacturing a long-lasting, wear-resistant cemented carbide-steel tool with a balanced joint strength and sufficient mechanical steel properties.

Based on these two incompatible process principles, this publication shows two different scientific approaches on how to manufacture a sound and strong cemented carbide-steel joint with a homogenous hardness of the steel by high-temperature vacuum brazing. Besides a common hot-work steel (1.2344) as an adequate joining partner for cemented carbide, a particular focus was put on the maraging steel 1.2709. Maraging steels contain high proportions of elements with a high oxygen affinity, such as titanium and aluminum [15], so that an oxide layer on the joining surface makes wetting by the liquid brazing material challenging [16]. An innovative concept will be introduced in this publication on how to make the maraging steel wettable at the example of cemented carbide/steel joints, but at the same time supplying a high joint quality as well as a homogenous and elevated hardness of the steel component. The strengthening of the copper-based fillet originates from the diffusion of nickel from the PVD-coating and the resulting strengthening of the copper-based matrix by solid solution strengthening and the precipitation hardening mechanism typical for Cu-Fe-Ni-alloys.

## 2 Materials

### 2.1 Cemented carbide (EMT 210)

As a joining partner for the steel, the cemented carbide grade EMT 210 with a grain size of ~0.8 µm was used. The

**Table 1** Chemical composition of cemented carbide in wt.-% (supplier: Extramet) [17]

WC	Co	Additional carbides
89.0	10.0	1.0

**Table 2** Chemical composition of used braze materials in wt.-% (supplier: Wesgo)

Braze material	Cu	Ge	Ni
Cu <sub>100</sub>	100.0	-	-
Cu <sub>87.75</sub> Ge <sub>12</sub> Ni <sub>0.25</sub>	87.75	12.0	0.25

chemical composition is displayed in Table 1. For the brazing tests, the EMT 210 was used in the form of a cylinder ( $\varnothing = 10$  mm,  $h = 5$  mm, Fig. 2 (left)). The EMT 210 cylinders were machined from a round bar by an electrical discharge machining (EDM) process and subsequently ground (600 pp) to free the joining surface from organics and oxide layers.

### 2.2 Braze material

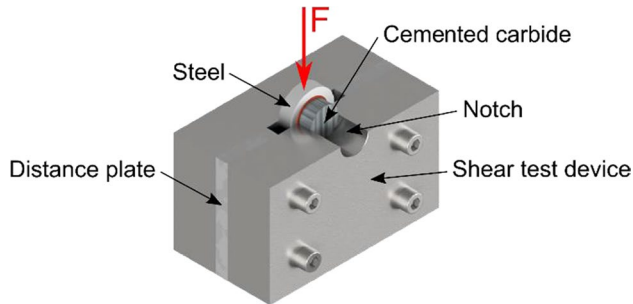
Pure copper and the copper-based filler metal Cu<sub>87.75</sub>Ge<sub>12</sub>Ni<sub>0.25</sub> were used in the brazing tests in the shape of a foil with a thickness of 100 µm and 75 µm, respectively, and a diameter of 12 mm (Table 2). The melting temperature of pure copper is 1083 °C. The recommended brazing temperature is 1100 °C. The solidus temperature of Cu<sub>87.75</sub>Ge<sub>12</sub>Ni<sub>0.25</sub> is 880 °C and the liquidus temperature is 975 °C. The recommended brazing temperature is between 1020 and 1060 °C.

### 2.3 Hot-work steel 1.2344 (X40CrMoV5-1), cold-work steel 1.2714 (55NiCrMoV7), and maraging steel 1.2709 (X3NiCoMoTi18-9-5)

As a joining partner for the cemented carbide, three different steel grades (1.2344, 1.2714, and 1.2709) were investigated (Table 3), which was reasoned by the different hardening mechanisms of such steels. For the brazing tests, the steel grades were machined into the shape of a cylinder ( $\varnothing = 20$  mm,  $h = 5$  mm). The steel cylinders were finely ground (1200 pp) on one side to free the joining surface from organics and oxide layers. All joining materials were cleaned in ethanol by ultra-sonic bath for 5 min before being positioned in the vacuum furnace chamber. A further explanation of the steel joining partners is conducted in Sections. 4.2 and 4.3 because an adaptation of the applied brazing process was conducted based on the corresponding metallurgical mechanisms of those steels.

**Table 3** Chemical composition of used steel grades in wt.-% (supplier: Abrams Premium Stahl and Deutsche Edelstahlwerke) [18–20]

Steel	Fe	C	Cr	Mo	V	Si	Ni	Co	Ti
1.2344	Bal	0.40	5.30	1.40	1.00	1.00	-	-	-
1.2714	Bal	0.55	1.10	0.50	0.10	-	1.70	-	-
1.2709	Bal	<0.03	-	5.00	-	-	18.00	10.00	1.00

**Fig. 1** Testing device used for shear strength determination

### 3 Experimental procedures

#### 3.1 Shear testing geometry

The samples were shear tested using a shear device set-up to assess the joint strength properties, as shown in Fig. 1. A steel cylinder is positioned in the gap of the shear strength test device and therefore can only be moved in the loading direction. The notch, which was eroded into the surface of the device, holds the joining partners in the correct position and guarantees an evenly distributed force transfer into the brazing seam along with the profile of the cemented carbide cylinder. The applied force was constantly raised with a rate of 1kN/s until the braze joint failed and the cemented carbide cylinder sheared off. The ultimate shear strength was then calculated by the quotient of the maximal measured force and the initial joining surface ( $A = 78.5 \text{ mm}^2$ ). The solidified brazing fillet outside the brazing seam was not removed before determining the shear strength of the braze joint. A statistically validated mean value for the shear strength was generated using the arithmetic mean of 3 shear samples per batch.

#### 3.2 PVD deposition of nickel coating

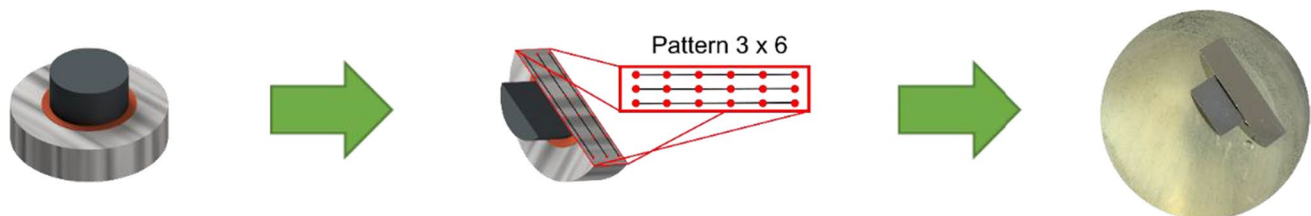
The maraging steel joining partners, except the benchmark brazements, were coated with a 5- $\mu\text{m}$ -thick nickel coating. Therefore, the joining surface was first ground (1200 pp) and polished with a diamond suspension (1  $\mu\text{m}$ ). Subsequently, the specimens were nickel-plated in a Metplas 20'' vacuum arc evaporator using a nickel cathode. Primarily, the joining surfaces were ion etched under vacuum ( $p = 3 \times 10^{-4}$  mbar, 100 A, – 1000 V bias voltage, 3 Ah) to free it from organics and oxide layers and other contaminations and to avoid the formation of new oxide layers. Subsequently, the steel samples were coated with an approximately 5- $\mu\text{m}$ -thick nickel layer (90 A, 30 V, 90 Ah).

#### 3.3 Hardness indentation

The measured hardness values were determined by a Vickers hardness tester (Stuers, Duramin 40) on a cross-section of the cemented carbide/steel joints applying a load of 1 kgf (kilogram-force) and a loading time of 15 s. A pattern of 18 indents evenly distributed over the cross-section of the steel part was applied (Fig. 2, middle). By evenly distributed over the whole cross-section is herein meant that the indents should be placed so that they cover the entire cross-section with a slight variation in the distance between them.

#### 3.4 SEM/EDS analysis

The SEM–EDS technique was used to analyze the microstructure of the braze joint and the base materials. The SEM used was a Jeol JSM-7001F using high-resolution field emission scanning electron microscopy (FE-SEM) with a thermal field emission cathode (Schottky). The mentioned SEM was used to investigate the joint microstructure and crack

**Fig. 2** Testing geometry (left), hardness measurement pattern (middle), and polished cross-section (right)

propagation and to determine the chemical composition of the occurring phases by EDS.

Due to the utilization of different material mechanisms, including the hardening mechanisms of the used steel grades, the manufacturing processes of the braze joints and the corresponding time–temperature profiles are further explained and displayed in the Section 4.

## 4 Results and discussion

If the steel component of a vacuum-brazed cemented carbide-transformation hardening tool steel joint should have adjustable and advanced mechanical properties, e.g., high tensile strength or hardness values, in theory, different scientific approaches could supply a satisfying solution:

### 4.1 Brazing at elevated temperatures

Compared to the widely spread induction brazing process, pre-hardened tool steel parts can be brazed to cemented carbide in a vacuum brazing process ( $p < 10^{-4}$  mbar) to obtain elevated hardness values of the steel component. The problem with that approach is that, in contrast to the induction brazing process, not only a small region but all joining partners are exposed comprehensively to the occurring temperatures. Usually, silver- and copper-based filler metals with liquidus temperatures over 750 °C are used for vacuum brazing [8]. The high temperatures and long dwell times, which are due to the sluggish heating and cooling behavior of vacuum furnaces, lead to microstructural changes in the used pre-hardened tool steel. These microstructural changes include the martensite relaxation, the dissolution of the secondary hardness carbides, and the re-transformation from martensite to ferrite and pearlite [6]. The approach to

manufacture cemented carbide/steel joints by vacuum brazing pre-hardened tool steel components to cemented carbide was not further pursued in this publication.

### 4.2 Integration of heat treatment of 1.2344 into brazing cycle

A second possibility to manufacture vacuum-brazed high-strength cemented carbide/transformation hardening tool steel joints with homogenous and elevated mechanical steel properties is integrating the heat treatment into the vacuum brazing process. This means that not only the steel but the whole joint, including the cemented carbide part, will undergo a steel heat-treatment process. Therefore, as it is marked in Fig. 3, the austenitization temperature of the 1.2344 must equal the brazing temperature. Thus, the recommended brazing temperature of the applied filler metal must approximately match the austenitization temperature of the steel in use, which is 1020–1060 °C for the 1.2344 [18].

Based on this requirement, the copper-based filler metals  $\text{Cu}_{100}$  and  $\text{Cu}_{87.75}\text{Ge}_{12}\text{Ni}_{0.25}$  from Table 2 were evaluated. A slightly higher austenitization temperature of 1100 °C was tolerated for the  $\text{Cu}_{100}$  due to the high melting point of pure copper of 1083 °C. Copper, as a chemical basis for both brazing foils, is known for reducing residual stresses caused by the CTE mismatch of steel and cemented carbide during the cooling phase [21]. The application of copper-based filler metals becomes essential when a quenching process is integrated into the brazing cycle, as it is the case with the integration of the heat treatment of the 1.2344 into a vacuum brazing cycle. The advantages and disadvantages of both filler metals regarding the intended application are listed in Table 4.

The time–temperature cycle applied to braze the cemented carbide joining partner to the hot-work steel

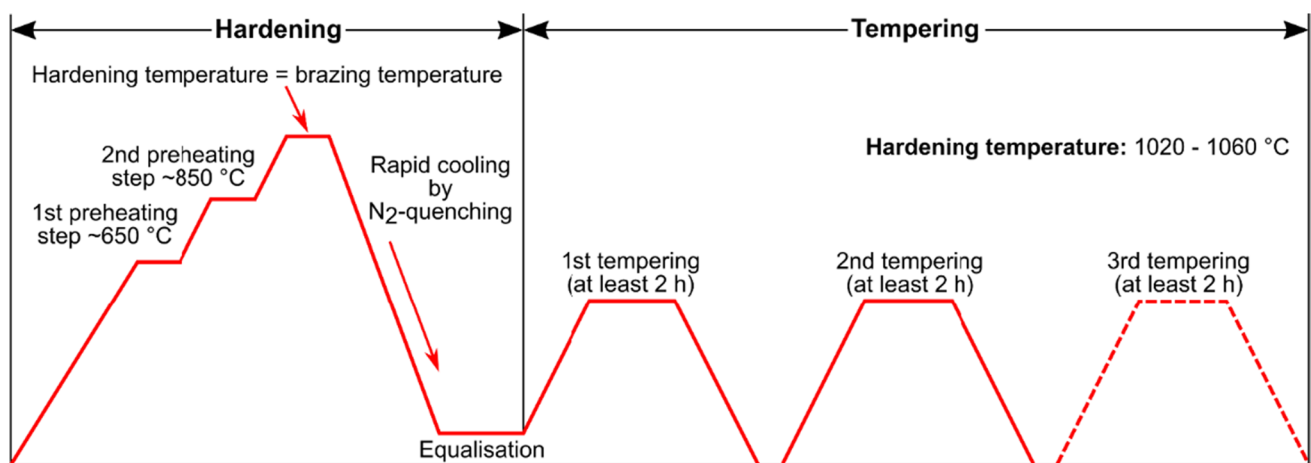


Fig. 3 Thermal cycle diagram of hot-work steel 1.2344 [18]

**Table 4** Advantages and disadvantages of pure copper and Cu<sub>87.75</sub>Ge<sub>12</sub>Ni<sub>0.25</sub> filler metal regarding the present application

Filler metal	Advantage	Disadvantage
Cu <sub>100</sub>	<ul style="list-style-type: none"> <li>• No elements, which tend to form hard and brittle phase</li> <li>• Optimal filler metal to reduce residual stresses [21]</li> </ul>	<ul style="list-style-type: none"> <li>• Brazing temperature (1100 °C) is higher than austenitization temperature (1020–1060 °C)</li> <li>• Higher temperatures can cause grain growth, which can negatively affect steel properties [22]</li> </ul>
Cu <sub>87.75</sub> Ge <sub>12</sub> Ni <sub>0.25</sub>	<ul style="list-style-type: none"> <li>• Brazing temperature equals recommended austenitization temperature (1020–1060 °C) [18]</li> </ul>	<ul style="list-style-type: none"> <li>• Forms germanium-rich interlayer between braze metal and cemented carbide</li> <li>• Not well-investigated system</li> </ul>

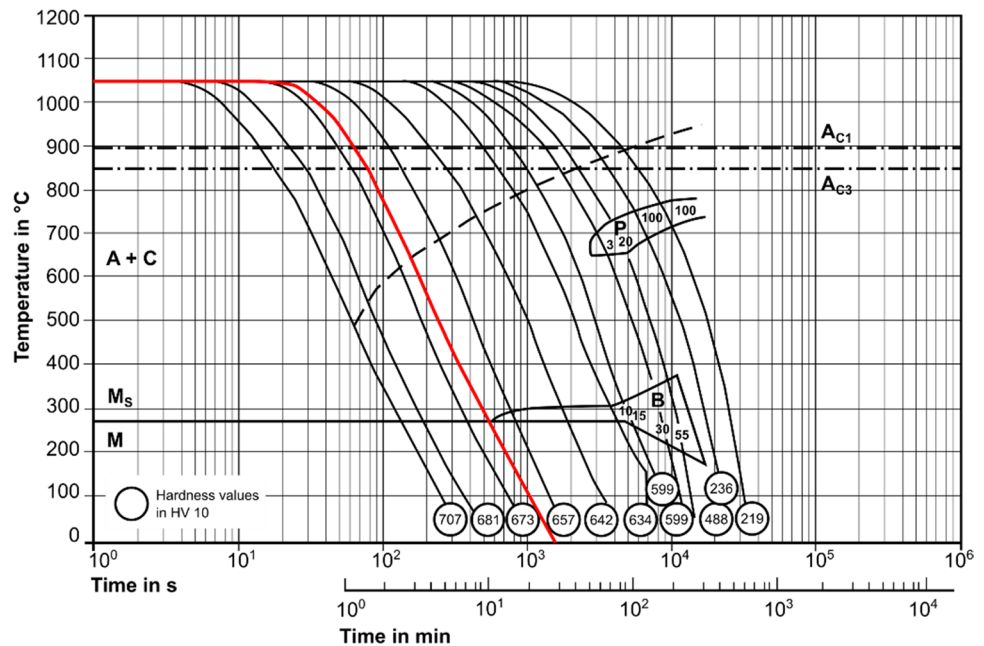
1.2344 needs to fulfill two requirements. On the one hand, it must supply an adequate brazing condition, including sufficient heating plateaus, high temperatures, long dwell times and low heating and cooling rates. On the other, it must ensure a comparable high cooling rate, respectively, quenching from the austenitization temperature to room temperature, which cannot fall below a specific value [18].

The continuous time–temperature-transformation diagram (TTT) (Fig. 4) predicts the occurring steel microstructure and macro hardness value of the 1.2344 hot-work steel in dependence of the cooling rate from austenitization temperature [18]. The red line in Fig. 4 marks the minimal possible cooling rate if an elevated hardness should be achieved and a formation of undesired intermediate phase mixtures should be avoided. A cooling time from austenitization temperature to room temperature of less than 1000 s (~ 16 min) needs to be achieved to supply an almost pure martensitic structure in the hot-work steel 1.2344 without the formation of bainite or pearlite.

Based on the previously explained requirements for a proper hot-work steel (1.2344) heat treatment (Fig. 3 and

Fig. 4), but at the same time with a focus on a high braze joint strength of at least 150 MPa and a high hardness level as well as an even distribution of the hardness within the steel component, a brazing process with an integrated heat treatment was developed. The displayed time–temperature diagram (Fig. 5) refers to the brazing tests conducted with pure copper as a filler material. In this context, a brazing temperature of 1100 °C was applied for 15 min. The time–temperature profile for the germanium-containing copper-based filler metal was conducted equivalently but with a brazing temperature of 1040 °C. All remaining process parameters were kept constant. A heating rate of 20 °C/min was set up to a temperature of 650 °C. At 650 °C, a heating plateau was initiated for 5 min. From 650 °C, a moderate heating rate of 10 °C/min was applied with the goal to supply a homogenous heat distribution within the joining partners. The brazing time of 15 min equaled the minimum dwell time of the austenitization temperature suggested by the steel supplier [18]. After the brazing interval, the specimens were cooled down by a controlled cooling rate of 50 °C/min to a temperature of 850 °C. As soon as

**Fig. 4** Time–temperature-transformation diagram of the hot-work steel 1.2344 [18]



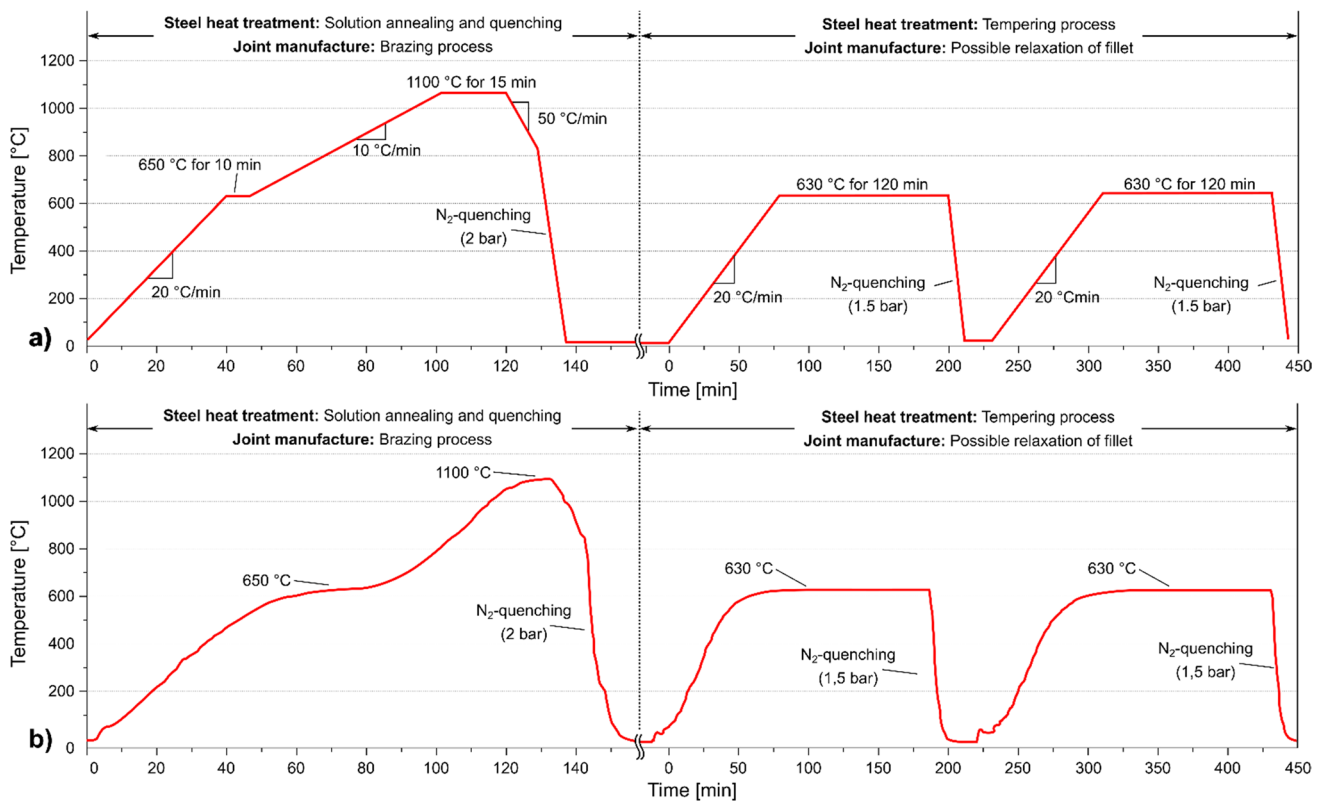


**Fig. 5** Theoretical (a) and actual (b) time–temperature profile of brazing process with pure copper at 1100 °C with an integrated hot-work steel heat treatment

the temperature reached 850 °C, the quenching process was initiated. N<sub>2</sub> was then injected into the furnace chamber with a pressure of 2 bar and a fan frequency of 2500 min<sup>-1</sup>. The quenching process was conducted from 850 °C after a controlled cooling from austenitization temperature instead of directly cooling down from 1100 °C. The deviation from the suggested heat treatment of the steel was conducted to reduce the thermal-induced mechanical tensions inside the joint. The joints were then tempered in the following heat treatment with a tempering temperature of 630 °C for two times two hours. The evaluation of the recorded time–temperature profile revealed a cooling time from 850 °C to room temperature of around 10 min, which is significantly lower than the prior determined maximal time window of 16 min regarding a proper heat treatment. In this context, a reference specimen was manufactured of the hot work-steel 1.2344 and the corresponding cemented carbide cylinder, which had the same size and consequently the same heating and cooling behavior as the introduced joining geometry (compare Fig. 2, left). The components were previously joined by spot-welding to guarantee a firm joint even at brazing temperature. A drill hole at the side of the steel cylinder reached from the surface to the core of the specimen. The temperature measured in the center of the steel specimen

was then the basis for the process regulation of the following brazing processes.

The brazing and tempering cycle displayed in Fig. 5 resulted in a mean shear strength of 17.1 MPa for the brazements conducted with pure copper ( $t_s = 100 \mu\text{m}$ ) as a filler material. The specimens brazed with Cu<sub>87.75</sub>Ge<sub>12</sub>Ni<sub>0.25</sub> featured a mean shear strength value of 18.2 MPa. The hardness level of the 1.2344 hot-work steel almost reached a mean hardness of 527.1 HV1 with a relatively low standard deviation of 17.1 HV1. The hardness level of the steel brazed with Cu<sub>87.75</sub>Ge<sub>12</sub>Ni<sub>0.25</sub> was determined with 494.0 HV1 ± 3.5 HV1. With regard to the threshold value of at least 150 MPa, the obtained shear strength values below 20 MPa did not meet the previously determined requirements at all, even though a sufficient hardening of the steel component was achieved with the heat treatment integration into the brazing process.

The focus of the microstructure analysis in the following was put onto the joints brazed with pure copper since the application of copper as a filler metal is state of the art and well researched. Figure 6 shows the microstructure of the joint, which was brazed according to the time–temperature profile displayed in Fig. 5. Contrary to the expectations, an almost continuous crack was present at the steel/fillet

interface after the brazing and tempering process. Due to the difference in CTEs, possible occurring cracks caused by the quenching process were assumed to be present at the interface between the cemented carbide and the copper fillet. Single voids between the cemented carbide and the fillet were visible along the brazing seam. In this context, the for cemented carbide/steel brazements with pure copper typical Fe-Co-phase (spectrum 1 in Fig. 6 and Table 5) is present at the cemented carbide/fillet interface and reaches from the cemented carbide into the copper-based fillet (spectrum 2 in Fig. 6 and Table 5). Still, the crack propagation at the interface between the hot-work steel 1.2344 and the copper fillet was predominant. In this context, the weakening mechanism “liquid metal embrittlement” (LME) was observed and can eventually be responsible for the crack formation at the steel/fillet interface. Low melting metals like copper diffuse into the grain boundaries of the base metal (Fig. 6) and cause a loss of ductility [23]. The loss of ductility combined with

high cooling rates respectively quenching might be responsible for the observed crack formation. The microstructure evaluation expected the joint to fail at the interface between the copper fillet and the hot-work steel surface after shear load application.

This assumption was confirmed by the following fracture mirror analysis (Fig. 7). After the shear tests were conducted, the copper fillet was present on both sides (Fig. 7, left). The steel-sided fracture mirror shows dark regions spread over the whole joining area, which have the same shade as the steel joining partner itself. The EDS analysis of those spots showed a chemical composition close to the one of the hot-work steel 1.2344 (Fig. 7, right). 86.4 wt.-% iron, 4.8 wt.-% chromium, 1.4 wt.-% vanadium, and 1.0 wt.-% silicon were measured, only present in the steel component. The red area (copper fillet) consisted mainly of copper (55.8 wt.-%) but also included iron (33.6 wt.-%) from the steel component and cobalt (3.4 wt.-%) from the cemented carbide joining

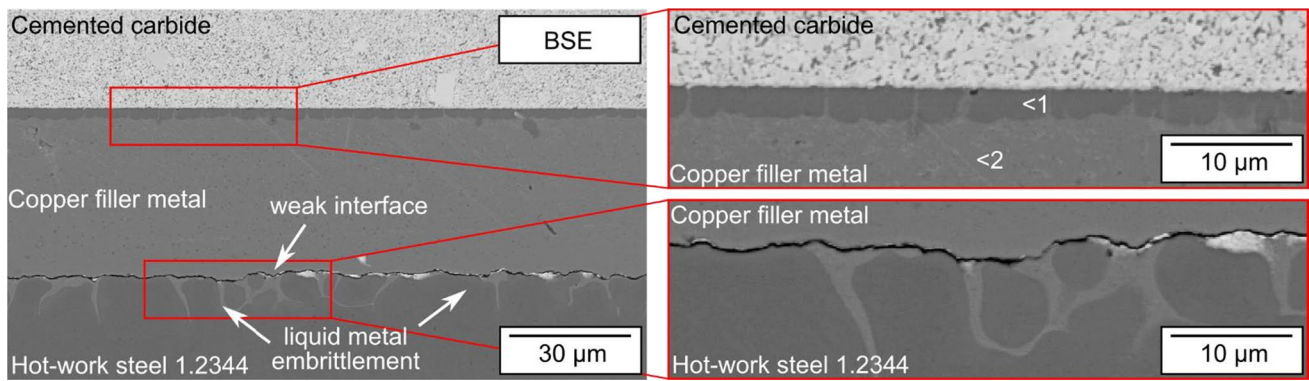


Fig. 6 Cemented carbide/steel joint microstructure brazed with corresponding cemented carbide/fillet and fillet/steel interfaces

Table 5 Chemical composition [in wt.-%] of characteristic phases of brazing seam from Fig. 6 by EDS spot analysis

Spot no	V	Cr	Fe	Co	Cu	W
1	0.5	3.3	55.8	25.1	8.9	6.4
2	-	-	1.5	0.5	98.0	-

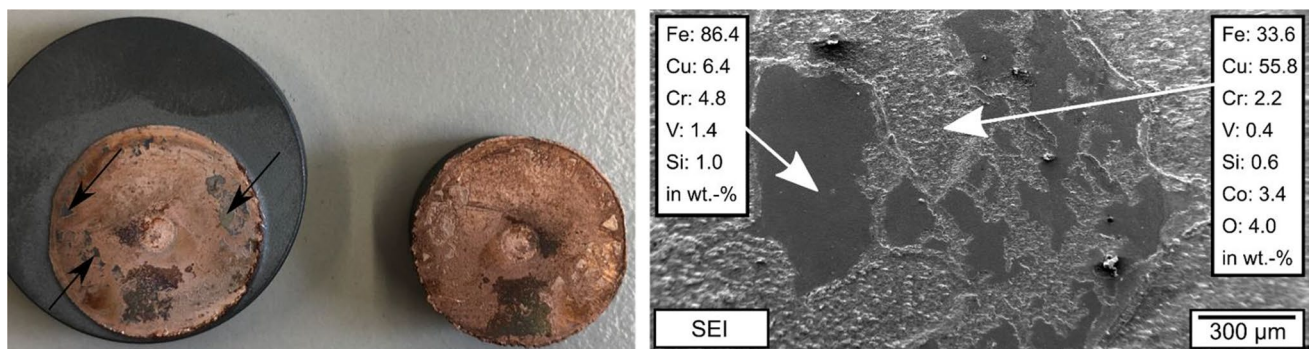


Fig. 7 Fracture mirror of failed cemented carbide/steel joint in macroscopic (left) and microscopic view (right)

partner. These results indicate that the joint failure occurred in the copper-rich fillet but also along the interface between the fillet and the steel.

Moreover, it was assumed that a poor wetting of the steel component by the copper filler metal was responsible for the formation of the weak interface and consequently for the shear strength values below 20 MPa. The bad wetting was attributed to an uneven heat distribution of the joining partners. Due to their smaller volume, the cemented carbide pieces were expected to be heated up quicker than the steel components. The copper filler metal would start to wet the cemented carbide and would be dragged away from the steel covering the sides of the cemented carbide cylinder. The small brazing gap width of ca. 50  $\mu\text{m}$  (Fig. 6) supports this theory since a 100- $\mu\text{m}$ -thick copper foil was applied for the brazing tests.

An adapted brazing cycle with an integrated steel heat treatment was developed based on the assumption of an insufficient heat distribution within the joining partners (Fig. 8a). A second heating plateau was established at 850  $^{\circ}\text{C}$  for 10 min. From 850  $^{\circ}\text{C}$ , the specimens were heated up with a heating rate of 5  $^{\circ}\text{C}/\text{min}$  to guarantee a homogenous heat distribution within the joining partners. After the dwell time of 15 min, the temperature

was decreased to a value of 1020  $^{\circ}\text{C}$ , which is the lowest recommended austenitization temperature according to the datasheet of the 1.2344 [18]. In this context, the controlled cooling was conducted with a cooling rate of 5  $^{\circ}\text{C}/\text{min}$  to decrease the occurring thermal induced mechanical stresses further. From 1020  $^{\circ}\text{C}$ , the temperature was regulated to 850  $^{\circ}\text{C}$  by 50  $^{\circ}\text{C}/\text{min}$  and then  $\text{N}_2$ -quenched to room temperature. Figure 8b shows the recorded time–temperature profile in the vacuum furnace.

According to Fig. 13, the adaption of the process parameters (compare column 1 to column 3) did not increase joint shear strength. To determine the influence of the quenching step on the joint shear strength, several benchmark brazing tests without a followed  $\text{N}_2$ -quenching step were conducted using pure copper as a filler metal. The specimens were brazed according to the brazing cycle in Fig. 8, but with free cooling from 850  $^{\circ}\text{C}$  instead of  $\text{N}_2$ -quenching. A maximal joint strength of  $186.5 \pm 13.5$  MPa was reached. A benchmark experiment with the same process parameters but with the application of the cold-work steel 1.2714, supplied a mean joint strength of  $192.0 \pm 14.0$  MPa. In this context, the measured shear strength values are in the range of those described in the literature for cemented carbide steel joints with copper as a filler metal [8].

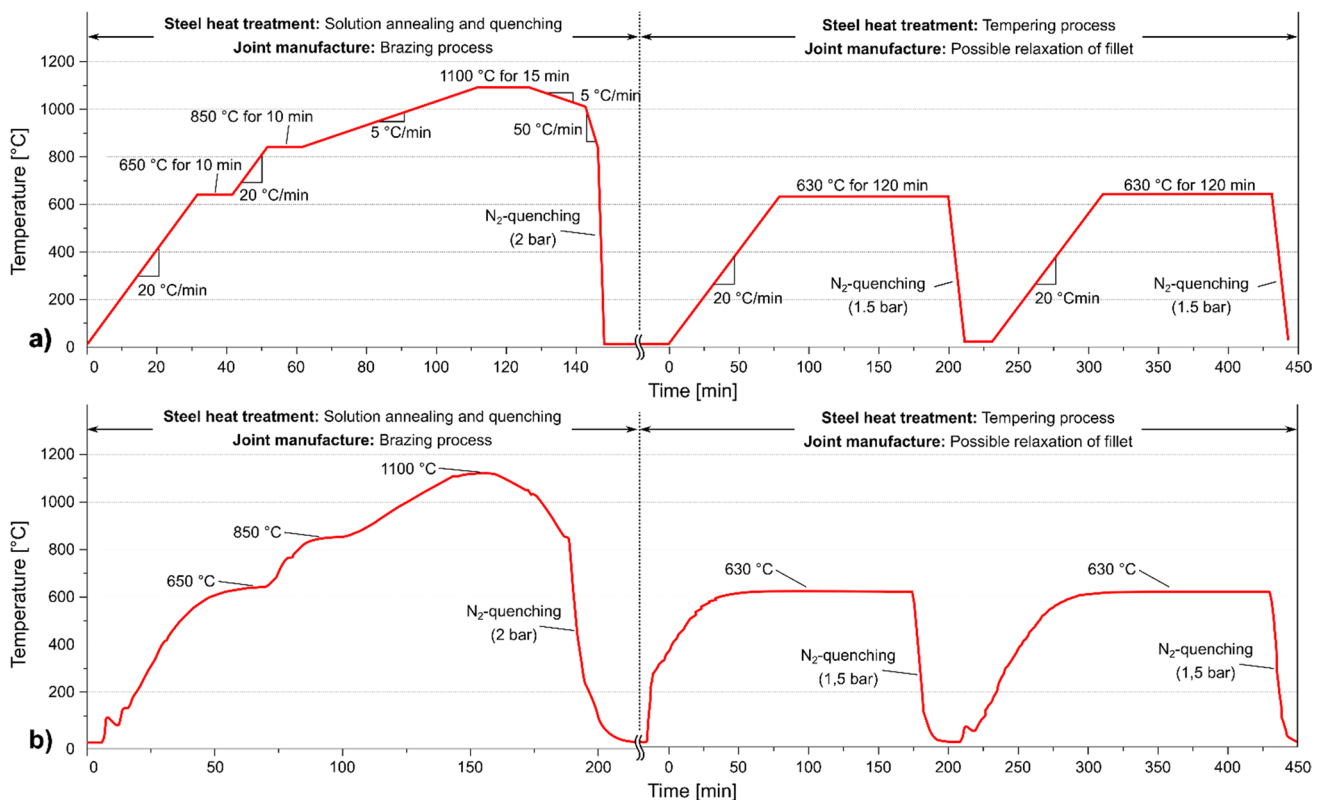


**Fig. 8** Theoretical (a) and recorded (b) time–temperature profile of brazing process with pure copper at 1100  $^{\circ}\text{C}$  with integrated hot-work steel heat treatment



Concluding, based on the previously displayed results, the integration of a transformation hardening steel heat treatment into a brazing process is no expedient approach, which provides the desired target hardness requirements of 400 and 440 HV1 and shear strength requirements of > 150 MPa. The N<sub>2</sub>-quenching, which is indispensable for achieving the required hardness level of the steel, has a very strong negative impact on the shear strength of the joint. Neither the pure copper nor the Cu<sub>87.75</sub>Ge<sub>12</sub>Ni<sub>0.25</sub> filler metal could reduce the occurring stresses caused by the applied rapid cooling rate. The occurring stresses shall be assumed to be even higher when the brazing geometry is scaled up to a higher specimen volume. Furthermore, an adapted brazing cycle (Fig. 8) with an additional heating plateau at 850 °C, a lower heating rate to brazing temperature of 5 °C/min, and a controlled cooling rate down to 1020 °C did not lead to acceptable bond strength values, either. Several benchmark experiments using free cooling proved that the copper system is generally suitable for manufacturing high-strength cemented carbide/steel joints. A further decrease of the cooling rate would lead to a deviation of the suggested proper steel heat treatment, which then again results in undesired intermediate steel phase mixtures like bainite and pearlite and a significant hardness loss according to the time–temperature–transformation diagram of the 1.2344 (Fig. 4) [18]. Thus, the technical limits of this process have been reached. No satisfying solution was found with this approach.

### 4.3 Integration of heat treatment of 1.2709 maraging steel into brazing cycle

Another approach to achieve a homogenous hardness level between 400 and 440 HV1 within the steel component and a shear strength of at least 150 MPa for cemented carbide/steel joints is the application of a maraging steel (e.g., 1.2709 in

Table 3 [19]) as a steel joining partner for cemented carbide. Maraging steels belong to the class of high-strength steels and differ from conventional transformation hardening cold-work, hot-work, and high-speed steels in their metallurgical hardening mechanism [15]. Maraging steels are high-alloy, low-carbon lath martensitic steels based on Fe and Ni with outstanding toughness values. In contrast to transformation hardening tool steels, the increase in strength and hardness of maraging steels is caused by the precipitation of intermetallic phases dispersed in the steel microstructure. After solution annealing at temperatures between 810 and 980 °C between 10 min and 1 h, a bcc martensite (lath martensite) with a hardness of 30–35 HRC is present at room temperature. In this context, the cooling rate from solution annealing to room temperature has a negligible influence from a nickel content > 10 wt.-% even for large components (Fig. 9, left). When tempering in the range between 350 and 600 °C (Fig. 9, right), the precipitation hardening mechanism occurs after only a few seconds and reaches its maximum effect after approx. 12 h. In practice, annealing times between 3 and 12 h are common. The intermetallic phases formed in the precipitation reaction described are Ni<sub>3</sub>Mo and Ni<sub>3</sub>Ti [24].

For the combined heat treatment-brazing process of non-austenitic steels, the CTE of the undercooled austenite and the volume change associated with the austenite–martensite transformation, including the volume expansion, are the critical factors for the development of thermal mismatch and residual stresses upon cooling, respectively. In the case of maraging steels, the produced lath martensite before precipitation hardening is generally much softer than the plate martensite of transformation-hardening steels. In addition, lath martensite can compensate large amounts of externally imposed stresses during the austenite-to-martensite transformation [26]. Furthermore, due to their chemical

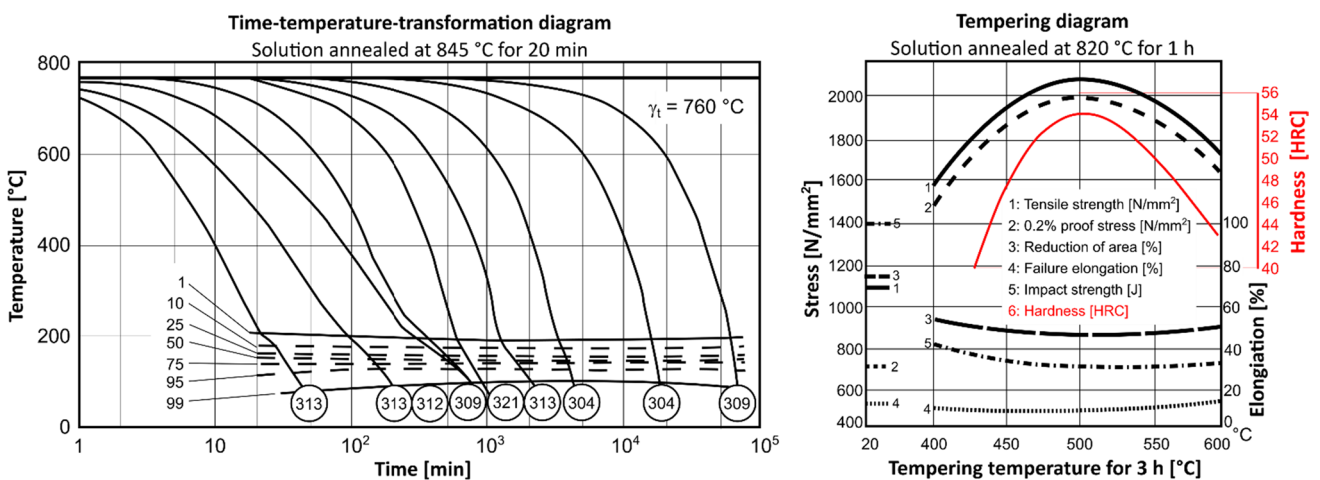


Fig. 9 Time–temperature–transformation diagram (left) and tempering diagram (right) of 1.2709 [24, 25]

**Table 6** CTEs of cold-work steel 1.2714, maraging steel 1.2709, and cemented carbide between 20 and 500 °C [18–20]

Material	1.2344	1.2714	1.2709	Cemented carbide
CTE [ $10^{-6}$ m/(mK)]	13.0	14.1	11.8	5.0–7.0

composition (e.g., 1.2709 in Table 3), the formation of a martensitic structure is independent of the cooling rate. This is a decisive factor, which supplies a significant advantage in brazing since the occurring thermal-induced joint stresses can be kept at a minimum. On this basis, the maraging steel 1.2709 was selected as a joining partner for cemented carbide. Moreover, due to its composition, the 1.2709 has a comparably low coefficient of thermal expansion (CTE) (Table 6) [19], which makes the 1.2709 superior to other common tool steels (e.g., 1.2714 [20]) as a joining partner for cemented carbide. Also, the tempering time of at least 3 h makes the brazing process very stable and applicable for batches with a high number and volume of tools.

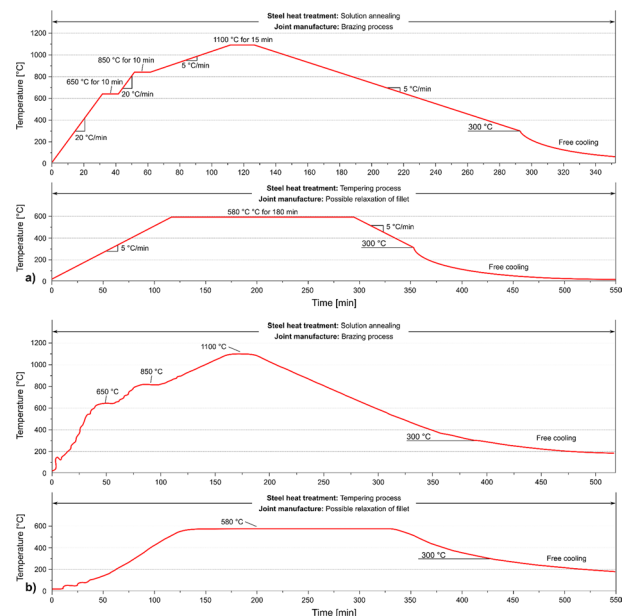
The mechanical properties of the 1.2709 are superior to those of the most transformation hardening tool steels and can be precisely adjusted by the tempering temperature (Fig. 9, right) [15]. It is visible in Fig. 9 (right) that the tensile strength and the 0.2% proof stress can significantly be increased by a tempering process conducted between 400 and 600 °C. The tensile strength and hardness values lie on the bell-shaped curve, where the maximum values are obtained at a tempering temperature of around 500 °C. The strength and hardness increase at temperatures between 20 and 500 °C is caused by the formation of  $\text{Ni}_3\text{Ti}$  and  $\text{Ni}_3\text{Mo}$  precipitates, which are coherently embedded into the martensitic steel microstructure and distort the lattice around them [27]. In turn, the strength and hardness reduction at temperatures of 500 °C and higher is caused by the dissolution of those intermetallic phases and a transformation from the martensitic to an  $\alpha$ -ferrite microstructure. According to the hardness bell curve of the 1.2709, the tempering of the cemented carbide/maraging steel joint should be conducted either at temperatures of around 420 °C or 600 °C to obtain the target hardness of  $\sim 420$  HV1 ( $\sim 42$  HRC).

For the brazing tests, the 1.2709 in a solution-annealed condition with a hardness of about  $\sim 340$  HV1 ( $\sim 32$  HRC) was used in the form of a cylinder ( $\varnothing = 20$  mm,  $h = 5$  mm). The 1.2709 cylinders were machined from a round bar by a turning process and subsequently ground (1200 pp) to free organics and oxide layers from the joining surface. Afterward, some of the steel samples were nickel-plated by a vacuum arc evaporator using pure nickel as a cathode to improve wetting, according to the research of Tillmann et al. [16]. The coating surfaces were primarily ion etched (100 A, 1,000 V bias voltage, 3 Ah) to obtain a high purity level by effectively removing possible surface oxides and other

contaminations. Then, the samples were directly coated with an approximately 5- $\mu\text{m}$ -thick nickel layer (90 A, 30 V, 90 Ah). Before the brazing process, all joining surfaces were purged with a cleaning cycle, utilizing ethanol.

The brazing process, which at the same time was the solution annealing process for the maraging steel 1.2709, is displayed in Fig. 10a (top). Besides the cooling phase, the brazing process was conducted the same way as the adapted brazement with the hot-work steel 1.2344 with a heating plateau at 650 and 850 °C (Fig. 8). Due to the lath martensite formation of maraging steels almost independent from the cooling rate, the cooling rate from brazing temperature to 300 °C was set up with 5 °C/min. From 300 °C, the specimens were cooled freely in vacuum. Intending to keep the occurring stresses of the firm bond at a minimum, the heating and cooling rate of the tempering process was 5 °C/min as well (Fig. 10a (bottom)). The selected tempering temperature of 580 °C was held for 3 h to obtain a homogenous hardness level between 400 and 440 HV1, and 42 and 44 HRC, respectively. The holding time of 3 h and the free cooling from 300 °C was initiated based on the steel manufacturer's recommendation [19]. The recorded time–temperature profile of the brazing and tempering process is displayed in Fig. 10b.

The braze joint microstructure of the brazement without the nickel coating of the steel joining surface is displayed in Fig. 11. The brazing gap with ca. 50  $\mu\text{m}$  is around half the width of the original copper foil thickness of 100  $\mu\text{m}$ . Consequently, the liquid filler metal was pushed out of the gap

**Fig. 10** Theoretical (a) and actual (b) brazing and solution annealing processes of maraging steel 1.2709 with subsequent tempering process with pure copper at 1100 °C

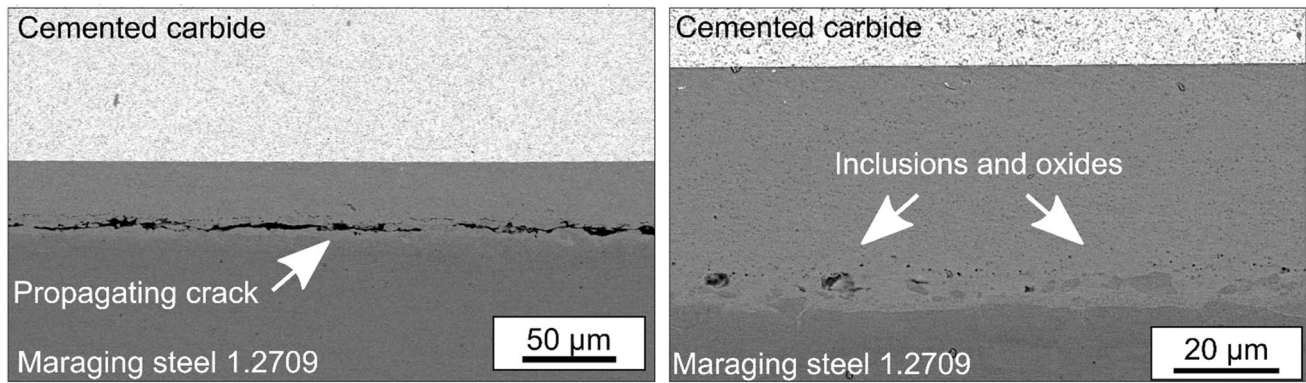


**Fig. 11** Cemented carbide-maraging steel brazed joint microstructure without nickel coating of steel joining surface with continuous propagating crack (left) and inclusion and oxides (right)

during the brazing process. A comprehensive observation of the joint reveals an almost continuously propagating crack at the maraging steel/fillet interface (Fig. 11, left). Small inclusions and pores surround the observed crack. It is assumed that these occurring inclusions and pores and consequently a bad wetting of the liquid copper originate from the oxide layers present on the maraging steel joining surface [28, 29]. An intact bond at a higher magnification is shown in Fig. 11 (right). The small nano-scaled oxides and pores are present at the cemented carbide/fillet interface and reach into the copper-rich matrix up to a depth of 10 µm. However, those occurring pores and oxides serve as critical points within the joint and result in a notch effect when the joint is loaded until joint failure. The evaluation of the sheared joint microstructure revealed a failure along the already existing crack at the maraging steel/fillet interface.

Despite the bad wetting of the maraging steel surface by the molten copper filler metal and the weak steel/fillet interface, the mean value of the joint shear strength was 151.6 MPa, which is in the range of cemented carbide/steel joints brazed with common silver-based filler metals and only slightly lower than the standard strength values for copper-based filler metals [8]. The corresponding and significantly high standard deviation of 47.5 MPa, ca. 30% of the measured mean shear strength, can be attributed to the uneven and inhomogeneous wetting of the steel by the filler metal. Therefore, a safe prediction of elevated shear strength values around 150 MPa cannot be assumed for the brazement without the nickel coating of the maraging steel joining surface.

In contrast to the brazement without the nickel coating and in accordance with the research of Tillmann et al. [16], a sound joint with high shear strength values was achieved by applying a 5-µm-thick PVD nickel coating on the joining surface of the maraging steel with the suggested brazing and heat treatment cycles from Fig. 10. In contrast to the carbide/steel braze joints with a transformation hardening

steel as a joining partner and pure copper as a filler metal, no continuous columnar Fe-Co–Cu phase has formed at the cemented carbide/copper fillet interface (compare Fig. 6 and Fig. 12b) [9]. Instead, dispersed Fe-Co–Cu precipitates have formed in the copper-rich fillet (Fig. 12a). The size and frequency of those globular phases decreased from the maraging steel to the cemented carbide. The diameters of the precipitates vary between about 100 nm and 3 µm. The chemical composition was determined with 58.0 wt.-% Cu, 24.0 Co wt.-%, and 18.0 wt.-% Fe using EDS analysis. In addition, the infiltration of the grain boundaries by the copper filler metal occurred only to a minor extent compared to the brazing tests without the nickel coating. Furthermore, a black seam of a few nanometers can be observed at the interface between the maraging steel and the fillet (Fig. 12c). It is assumed that the incomplete wetting is caused due to previous oxide layers on the joining surface of the maraging steel.

The shear strength of the brazed joint was  $326.5 \text{ MPa} \pm 17.7 \text{ MPa}$  (Fig. 13, column 7). The strength increase of more than 50% is explained by solid solution strengthening of the copper-rich fillet matrix (1.0 wt.-% Fe, 1.2 wt.-% Co, 1.0 wt.-% Ni, and 96.8 wt.-% Cu) by nickel diffusion from the PVD coating and on the other hand, by a precipitation hardening typical for Cu-Ni–Fe alloys [30]. With increasing temperature, the Cu-Ni-phase can dissolve iron of up to 5 wt.-%. In this case, iron diffuses from the maraging steel into the fillet. The copper-based copper-nickel solid solution is supersaturated with iron and precipitates finely dispersed iron-based particles when heated below the solubility line, causing a change in physical and mechanical properties. The maximum hardness of a Cu-Fe–Ni alloy is reached at an austenitization temperature of 990 °C at a nickel content of 10 wt.-%, an iron content of 1.96 wt.-%, and an annealing time of 2 h at 600 °C [30].

The hardness of the maraging steel joining partner was  $426.6 \pm 6.0 \text{ HV1}$  (Fig. 13, columns 6 and 7). Therefore, it can be stated that the hardening mechanism worked

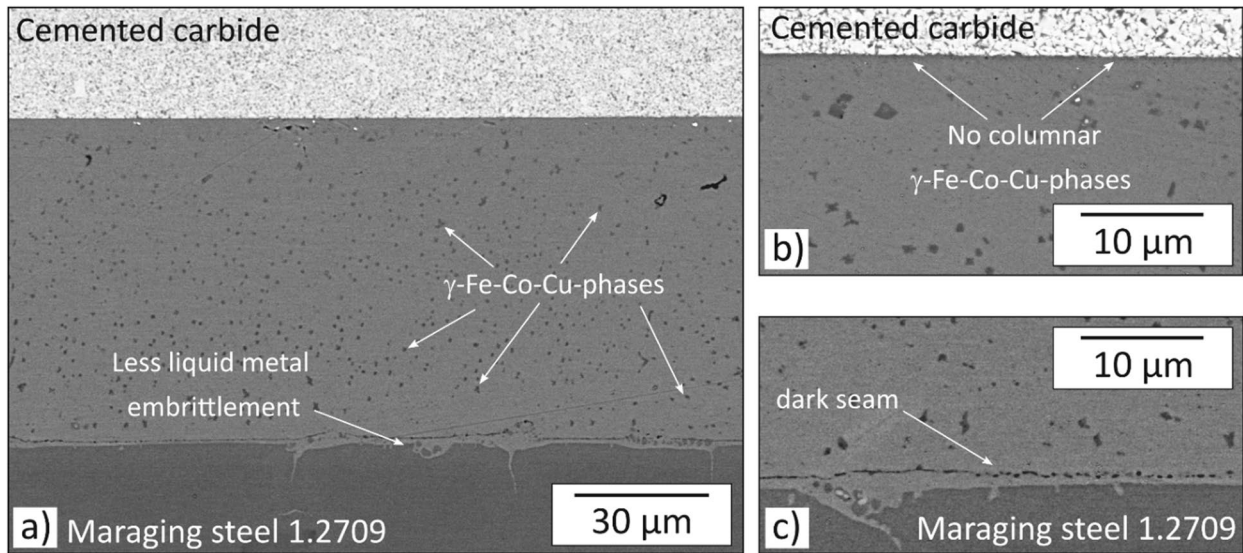


**Fig. 12** Cemented carbide/maraging steel braze joint microstructure with nickel coating of steel joining surface with **a** joint overview, **b** cemented carbide/fillet interface, and **c** fillet/steel interface

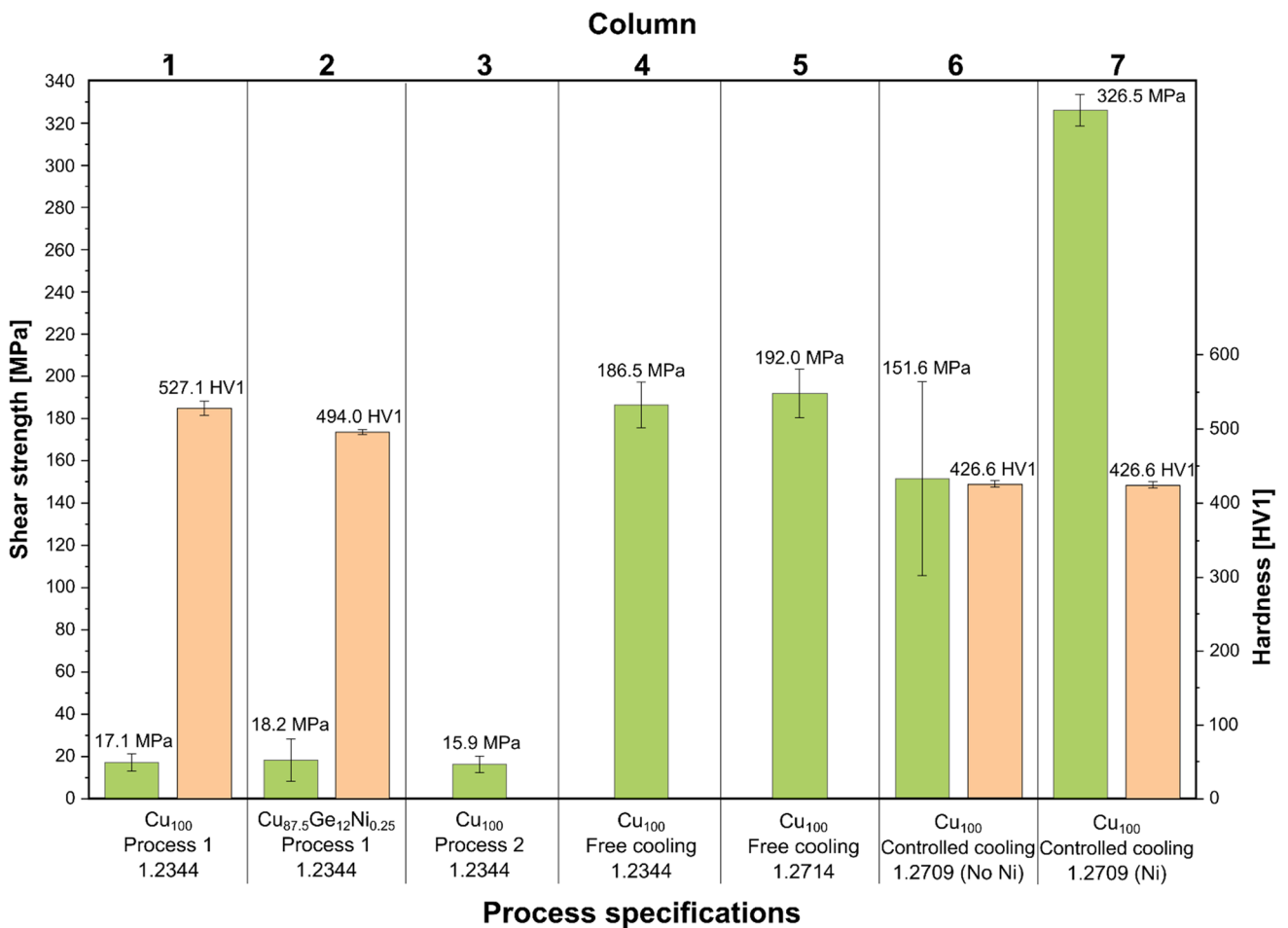


**Fig. 13** Joint shear strength and steel hardness values of different brazing cycles with integrated steel heat treatment

precisely, even though the recommended solution annealing temperature of the maraging steel was exceeded by ca. 250 °C. In this context, it was assumed that the nickel coating has no significant effect on the hardening mechanism of the maraging steel. Therefore, the values for the steel hardness in columns 6 and 7 in Fig. 13 are the same. The crack after joint failure mainly propagated at the fillet/maraging steel interface along the dark seam visible in Fig. 12c. The assumption is made that the oxides, which the ion etching process could not completely remove before the PVD nickel coating, weakened the joint and favored the crack propagation at the fillet/steel interface.

## 5 Conclusions

This paper evaluated the integration of three different steel heat treatment processes into a brazing process for cemented carbide/steel joints using copper-based filler metals. Whereas the quenching process had a significant negative impact on the joint quality, it was not required when the precipitation hardening tool steel 1.2709 was applied as a steel joining partner. Cemented carbide/steel joints with an outstanding joint shear strength of  $326.5 \text{ MPa} \pm 17.7 \text{ MPa}$  and a homogenous hardness of the steel joining partner could be supplied when the maraging steel grade 1.2709 was used. The main findings are summarized in the following:

- 1) The quenching process required for the hardening mechanism of the applied tool steel 1.2344 had a massive negative influence on the cemented carbide/steel joint shear strength. The joint shear strength was reduced by 169.4 MPa from 186.5 to 17.1 MPa compared to a benchmark brazing with vacuum cooling.
- 2) The application of a maraging steel as a cemented joining partner led to a significantly higher joint quality due to the hardening mechanism independent from the cooling rate and the consequently lower residual stresses after a controlled cooling with a rate of 5 °C/min.
  - a. The joint shear strength of cemented carbide maraging steel joints without a nickel coating of the steel joining surface was moderate with a value of 151.6 MPa, but with a massive standard deviation of 47.5 MPa. The for copper-based filler metals, comparable low shear strength and the high standard deviation were caused by the bad connection at the fillet/maraging steel interface originating from an oxide layer formation at the maraging steel surface.
  - b. The application of a nickel layer on the maraging steel joining surface ensured the wetting of the maraging steel joining surface and was responsible for a sound joint and a significantly high shear strength value of 326.5 MPa with a low standard deviation of 17.7 MPa.
  - c. The integration of the maraging steel heat treatment into a brazing process can be classified as successful since the aimed hardness level of 420 HV1 was precisely reached with a homogenous hardness level of  $426.6 \pm 6.0 \text{ HV1}$ .
- 3)  $\gamma$ -Fe-Co-phases in the copper-rich matrix of the fillet and the solid solution hardening of the copper-rich matrix by nickel diffusion from the nickel coating are responsible for the mechanical strengthening of the fillet and consequently for the increase in joint shear strength.

**Funding** Open Access funding enabled and organized by Projekt DEAL.

## Declarations

**Conflict of interest** The authors declare no competing interests.

**Open Access** This article is licensed under a Creative Commons Attribution 4.0 International License, which permits use, sharing, adaptation, distribution and reproduction in any medium or format, as long as you give appropriate credit to the original author(s) and the source, provide a link to the Creative Commons licence, and indicate if changes were made. The images or other third party material in this article are included in the article's Creative Commons licence, unless indicated otherwise in a credit line to the material. If material is not included in the article's Creative Commons licence and your intended use is not permitted by statutory regulation or exceeds the permitted use, you will need to obtain permission directly from the copyright holder. To view a copy of this licence, visit <http://creativecommons.org/licenses/by/4.0/>.

## References

1. Jiang C, Chen H, Wang Q et al (2016) Effect of brazing temperature and holding time on joint properties of induction brazed WC-Co/carbon steel using Ag-based alloy. *J Mater Process Technol* 229:562–569. <https://doi.org/10.1016/j.jmatprotec.2015.09.044>
2. Schimpfermann M, Wiehl G, Magin M, et al. (2019) Fundamental study on the tempered state of steel blades influenced by the brazing process parameters for joining of hard metals to saw blades. In: *Brazing, high temperature brazing and diffusion bonding - LÖT 2019*, Düsseldorf
3. Stahlhut C (2011) *Laserstrahl-löten von Stahl und Hartmetall für Laserstrahl-löten von Stahl und Hartmetall für zerspanende Werkzeuge mit definierter Schneide*, Hannover
4. Enke CG (1975) *Induktionserwärmung. (Härten - Glühen Schmelzen - Löten - Schweißen.)* G. Benkowsky . 3. Aufl. (1973). 268 S., 277 Abb. und 25 Tab. VEB Verlag Technik, Berlin/DDR - geb.: 16,- DM. *Materials and Corrosion* 26:91. <https://doi.org/10.1002/maco.19750260128>
5. Tillmann W, Lehmert B, Wojarski L, et al. (2018) Investigation of CuTi, CuNiSi and CuNiSiB alloys for brazing applications. *Proceedings IBSC*

6. Lappe V (2014) *Warmebehandlung des Stahls: Grundlagen, Verfahren und Werkstoffe*, 11. Aufl. Verlag Europa Lehrmittel
7. Sui Y, Luo H, Lv Y et al (2016) Influence of brazing technology on the microstructure and properties of YG20C cemented carbide and 16Mn steel joints. *Weld World* 60:1269–1275. <https://doi.org/10.1007/s40194-016-0374-0>
8. Zhang XZ, Liu GW, Tao JN et al (2017) Vacuum brazing of WC–8Co cemented carbides to carbon steel using pure Cu and Ag–28Cu as filler metal. *J Mater Eng Perform* 26:488–494. <https://doi.org/10.1007/s11665-016-2424-6>
9. Amelzadeh M, Mirsalehi SE (2019) Dissimilar vacuum brazing of cemented carbide to steel using double-layer filler metals. *J Manuf Process* 47:1–9. <https://doi.org/10.1016/j.jmapro.2019.09.015>
10. Chen H, Feng K, Xiong J et al (2013) Characterization and stress relaxation of the functionally graded WC–Co/Ni component/stainless steel joint. *J Alloy Compd* 557:18–22. <https://doi.org/10.1016/j.jallcom.2012.12.152>
11. Zhang X, Liu G, Tao J et al (2018) Brazing of WC–8Co cemented carbide to steel using Cu–Ni–Al alloys as filler metal: microstructures and joint mechanical behavior. *J Mater Sci Technol* 34:1180–1188. <https://doi.org/10.1016/j.jmst.2017.11.040>
12. Weise W, Koschlig M, Herzog H, et al. (1998) Einsatz innovativer Lote in der Schneidtechnik. In: DVS Media GmbH (ed) *Hart- und Hochtemperaturloten und Diffusionsschweien: Vortrage und Posterbeitrage des 5. Internationalen Kolloquiums in Aachen vom 16. bis 18. Juni 1998 : Lectures and posters of the 5th International Conference taking place in Aachen on 16th to 18th June 1998, Brazing, high temperature brazing and diffusion welding*, Verl. fur Schweien und Verwandte Verfahren DVS-Verl., Dusseldorf, pp 62–67
13. Chiu LH, Wang HF, Huang CP et al (2008) Effect of brazing temperature on the microstructure and property of vacuum brazed WC–Co and carbon steel joint. *AMR* 47–50:682–685. <https://doi.org/10.4028/www.scientific.net/AMR.47-50.682>
14. Amirnasiri A, Parvin N, Haghshenas MS (2017) Dissimilar diffusion brazing of WC–Co to AISI 4145 steel using RBCuZn–D interlayer. *J Manuf Process* 28:82–93. <https://doi.org/10.1016/j.jmapro.2017.06.001>
15. Davis JR (2001) *Properties and selection: Irons, steels and high-performance alloys*, [10. ed.], 6. print. ASM handbook, / prepared under the direction of the ASM International Handbook Committee; Vol. 1. ASM International, Materials Park, Ohio
16. Tillmann W, Henning T, Boretius M (2019) Effect of the dwell time on the microstructure and tensile strength of vacuum-brazed tool steels using BNi-2 filler metal. *Weld World* 63:1477–1488. <https://doi.org/10.1007/s40194-019-00734-z>
17. Extramet (2021) EMT 210 Data sheet. Accessed 16 Aug 2021
18. Dorrrenberg Edelstahl (2021) 1.2344 Data sheet: X40CrMoV5–1. <https://www.doerrenberg.de>. Accessed 16 Aug 2021
19. Dorrrenberg Edelstahl (2021) 1.2709 Data sheet: X3NiCo–MoTi18–9–5. <https://www.doerrenberg.de>. Accessed 16 Aug 2021
20. Dorrrenberg Edelstahl (2021) 1.2714 Data sheet: X55NiCrMoV7. <http://www.dorrenberg.de>. Accessed 16 Aug 2021
21. Schimpfermann M, Schnee D (2020) *Brazing in the tool manufacturing industry*
22. Lima Filho VX, Barros IF, Abreu HFG (2017) Influence of solution annealing on microstructure and mechanical properties of maraging 300 steel. *Mat Res* 20:10–14. <https://doi.org/10.1590/1980-5373-MR-2016-0257>
23. Kamdar MH (1983) Liquid metal embrittlement. In: *Embrittlement of engineering alloys*, vol 25. Elsevier, pp 361–459
24. Davis JR (2007) *Heat treating*, [10. ed.], 8. print. ASM handbook, / prepared under the direction of the ASM International Handbook Committee; Vol. 4. ASM International, Materials Park, Ohio
25. Bohler (2021) *Maraging high strength steel: W720*. <https://www.boehler-edelstahl.com>. Accessed 16 Aug 2021
26. Loewy S, Hjordt L, Rheingans B, Mittemeijer E (2016) Modulated formation of lath martensite: Influence of uniaxial compressive load and transformation-induced plasticity. *Acta Mater* 109:46–54. <https://doi.org/10.1016/j.actamat.2016.02.047>
27. Shimizu K, Okamoto H (1971) Transmission electron microscopy study of strengthening precipitates in 18% Ni maraging steel. *Trans JIM* 12:273–279. <https://doi.org/10.2320/matertrans1960.12.273>
28. Klein IE, Yaniv AE, Sharon J (1983) The mechanism of oxidation of Fe–Ni–Co alloys; the role of Ti and Mo. *Appl Surf Sci* 14:351–358. [https://doi.org/10.1016/0378-5963\(83\)90048-X](https://doi.org/10.1016/0378-5963(83)90048-X)
29. Berry RD (1965) *Joining 18 percent nickel maraging steels by brazing*. *Welding and metal fabrication*:93–95
30. Dies K (2014) *Kupfer und Kupferlegierungen in der Technik*, [Auflage 1967]. Springer Verlag, Berlin, Heidelberg

**Publisher's note** Springer Nature remains neutral with regard to jurisdictional claims in published maps and institutional affiliations.